

# Selective Nuclear Magnetic Resonance Experiments for Sign-Sensitive Determination of Heteronuclear Couplings: Expanding the Analysis of Crude Reaction Mixtures

Guilherme Dal Poggetto,\* João Vitor Soares, and Cláudio F. Tormena



Cite This: *Anal. Chem.* 2020, 92, 14047–14053



Read Online

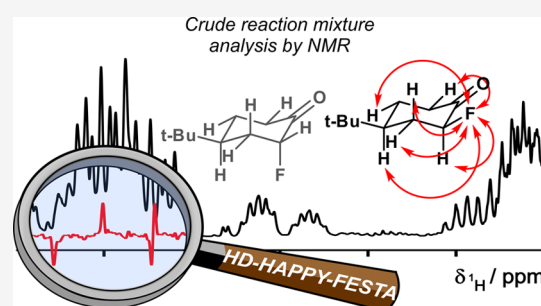
ACCESS |

Metrics & More

Article Recommendations

Supporting Information

**ABSTRACT:** State-of-the-art nuclear magnetic resonance (NMR) selective experiments are capable of directly analyzing crude reaction mixtures. A new experiment named HD-HAPPY-FESTA yields ultrahigh-resolution total correlation subspectra, which are suitable for sign-sensitive determination of heteronuclear couplings, as demonstrated here by measuring the sign and magnitude for proton–fluorine couplings ( $J_{\text{HF}}$ ) from major and minor isomer products of a two-step reaction without any purification. Proton–fluorine couplings ranging from 51.5 to  $-2.6$  Hz could be measured using HD-HAPPY-FESTA, with the smallest measured magnitude of 0.8 Hz. Experimental  $J_{\text{HF}}$  values were used to identify the two fluoroketone intermediates and the four fluoroalcohol products. Results were rationalized and compared with the density functional theory (DFT) calculations. Experimental data were further compared with the couplings reported in the literature, where pure samples were analyzed.



## INTRODUCTION

The incorporation of even a single fluorine atom in a molecule can affect its physical and chemical properties.<sup>1,2</sup> In drugs, fluorination has shown to improve metabolic stability and membrane permeation and increase binding affinity. Several examples of fluorinated compound synthesis in the literature<sup>3–6</sup> reflect the ever-growing interest in the discovery of new fluorinated drug candidates by the pharmaceutical industry.<sup>7,8</sup> Solution-state nuclear magnetic resonance (NMR) is arguably the most useful nondestructive spectroscopy technique for the analysis and characterization of chemical reaction products. Typically, these products are purified by physical separation methods (e.g., chromatography and recrystallization) in many manual steps before NMR analysis.<sup>9</sup> These time-consuming, resource-intensive, and often tedious practices can sometimes be avoided by analyzing the intact reaction mixture—either to bypass the necessity of difficult component separation or to have an extra source of information before isolation. Mixture analysis by NMR has been used successfully in the past for the analysis of natural products,<sup>10,11</sup> beverages,<sup>12,13</sup> pharmaceutical formulations,<sup>14,15</sup> among others, yet it is still a cumbersome task.

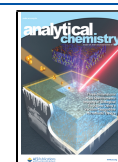
Chemical and structural insights are typically extracted from <sup>1</sup>H NMR spectra in the form of chemical shifts ( $\delta$ ) and scalar couplings ( $J$ ), but for complex mixtures, this information is severely obscured by signal overlap. It is also possible to obtain <sup>19</sup>F NMR spectra (when this is available in a molecule), which has a much larger frequency dispersion ( $\sim 500$  ppm) in comparison with the <sup>1</sup>H spectra ( $\sim 10$  ppm) and a far rarer

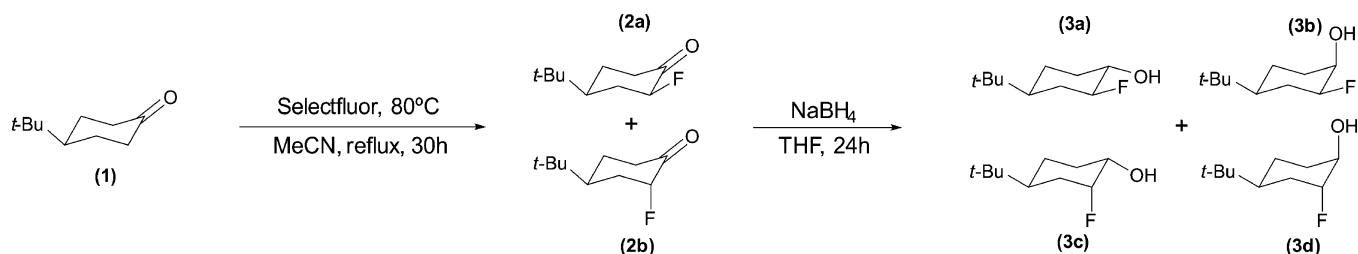
signal overlap.<sup>16</sup> Although <sup>19</sup>F NMR is used successfully for mixture analysis,<sup>17–20</sup> fluorine spectra contain insufficient information, unlike <sup>1</sup>H spectra, and therefore are not normally used for characterization but to probe various interactions,<sup>2,20–23</sup> commonly by observing the changes in signal chemical shift and relaxation. One way to take advantage of the spectral sparsity of <sup>19</sup>F to unambiguously assign the atomic connectivity, while still observing the more informational <sup>1</sup>H spectra, is by using 1D fluorine-edited selective TOCSY acquisition (FESTA).<sup>24,25</sup> In FESTA, only the <sup>1</sup>H signals that are in a spin system coupled to a selected fluorine nucleus are observed through magnetization transfer, that is, TOfal Correlation Spectroscopy (TOCSY).<sup>26</sup> Various 2D NMR experiments, such as hetero-COSY,<sup>27</sup> heteronuclear single quantum coherence-TOCSY (HSQC-TOCSY),<sup>28,29</sup> and more,<sup>30,31</sup> also give useful molecular knowledge of fluorinated species, but these usually have long experiment duration and are limited for high-concentration-dynamic-range mixtures,<sup>14</sup> as opposed to 1D-selective NMR experiments,<sup>32–34</sup> which can be used to observe signals coming from low-concentration components of complex matrixes. For the FESTA family of experiments, all <sup>1</sup>H signals observed belong to the same spin

Received: July 13, 2020

Accepted: September 14, 2020

Published: September 14, 2020



Scheme 1. Reactions Described in this Paper<sup>a</sup>

<sup>a</sup>The first step describes the experimental conditions for the  $\alpha$ -fluorination reaction of 4-*tert*-butyl-cyclohexanone (1), generating both fluorinated ketone isomers, 2a and 2b, at a ratio of 4.2/1.0, respectively. The second step describes the condition for the ketone reduction from the crude reaction product of the first step, generating simultaneously all four fluorinated alcohol isomers, 3a, 3b, 3c, and 3d, at a ratio of 9.1/4.8/2.8/1.0, respectively. The relative proportion of the products in each reaction step was measured by integration of the signals in the <sup>1</sup>H-decoupled <sup>19</sup>F spectra (Figure 3)

system connected to a selected <sup>19</sup>F nucleus. It is thus possible to obtain all <sup>1</sup>H chemical shifts ( $\delta_{\text{H}}$ ) and homonuclear <sup>1</sup>H–<sup>1</sup>H ( $J_{\text{HH}}$ ) and heteronuclear <sup>1</sup>H–<sup>19</sup>F ( $J_{\text{HF}}$ ) couplings, given that the signals are well-resolved. Fluorine decoupling can declutter the partial spectra even further; however, there are still difficulties in using FESTA to measure  $J_{\text{HF}}$ , which are abundant in structural and conformational information.<sup>35</sup> These couplings are frequently used as a diagnostic tool for full characterization.<sup>29,36</sup> In contrast, with <sup>2</sup> $J_{\text{HH}}$ , germinal <sup>2</sup> $J_{\text{HF}}$  are large and positive. Vicinal <sup>3</sup> $J_{\text{HF}}$  can be both positive and negative, with a larger span of magnitudes compared to <sup>3</sup> $J_{\text{HH}}$ . Longer-range <sup>*n*</sup> $J_{\text{HF}}$  are also quite common. Frequently, the magnitudes of  $J_{\text{HH}}$  and  $J_{\text{HF}}$  are similar within the multiplet structure, making them hard to be distinguished from one another. Suppressing the effects of homonuclear couplings can be a very effective way of measuring the magnitude of heteronuclear couplings.<sup>37–39</sup> This can be achieved with “ultrahigh-resolution”<sup>40–42</sup> pure shift NMR methods<sup>43–45</sup> in which heteronuclear couplings are left unaffected. Unfortunately, pure shift methods alone are hopeless to analyze but the simplest mixtures, as most complex mixtures have wall-to-wall peaks. Recently, an experiment combining selective spin echo (SSE)-TOCSY with Pure Shift Yielded by CHirp Excitation (PSYCHE)<sup>40</sup> was proposed,<sup>10</sup> allowing the analysis of high-dynamic-range reaction mixtures. This method simplifies the <sup>1</sup>H spectrum by only observing the subspectra from the <sup>1</sup>H spin systems of interest (as in FESTA) and uses pure shift NMR to remove the effects of  $J_{\text{HH}}$ . As useful these may be, neither FESTA nor SSE-TOCSY-PSYCHE is sensitive to the sign of couplings. Only when both the magnitude and the sign are available, this property can be used to determine the relative configuration above any doubt.<sup>36</sup> For <sup>*n*</sup> $J_{\text{HF}}$ , the sign and magnitude are also crucial to understanding the electronic interactions behind scalar coupling transmission mechanisms.<sup>46,47</sup>

Here, we propose a combination of homonuclear decoupling with a modified MODulated echo (MODO)-FESTA<sup>25</sup> for the sign-sensitive determination of heteronuclear <sup>*n*</sup> $J_{\text{HF}}$  in complex mixtures, adding a powerful tool to the FESTA family of experiments. This new method, named Homonuclear Decoupled Heteronuclear AntiPhase Permuted modulated echo Yielding Fluorine-Edited Selective TOCSY Acquisition (HD-HAPPY-FESTA), was used to obtain all relevant  $J_{\text{HF}}$ , with ease and high precision, for the two-step reaction (Scheme 1) of the formation of fluorinated alcohol isomers with no purification before NMR analysis. While conventional (Figure 1a) and pure shift (Figure 1b) <sup>1</sup>H spectra completely

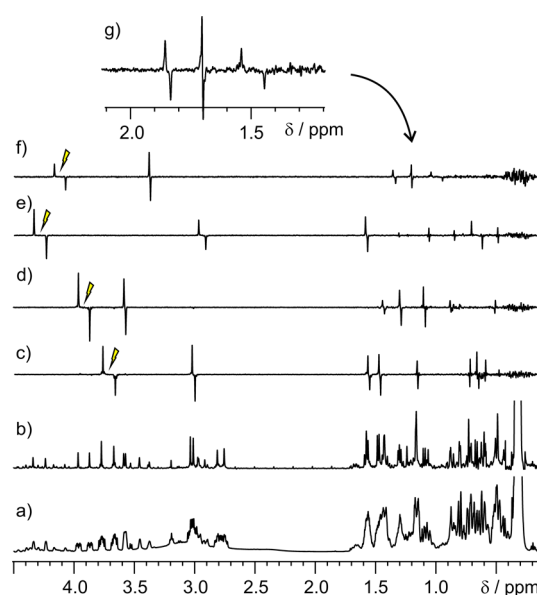


**Figure 1.** 500 MHz (a) conventional, (b) PSYCHE, and (c–f) HD-HAPPY-FESTA (isotropic mixing time of 150 ms) <sup>1</sup>H spectra of a crude reaction mixture from the reduction of ketones 2a and 2b in CDCl<sub>3</sub>. Ultrahigh-resolution sign-sensitive antiphase heteronuclear total correlation spectra of alcohols: (c) 3a; (d) 3b; (e) 3c; and (f) 3d, respectively. Molecular structures are shown in Scheme 1. (g) is the expansion of (f) between 1.2 and 2.1 ppm. Lightning bolts in (c–f) indicate chemical shifts of band-selective <sup>1</sup>H pulses, selected using 24.4 ms REBURP pulses (<sup>1</sup>H bandwidth of 200 Hz). A flip angle ( $\beta$ ) of 24° and 80 data chunks of 12.5 ms duration were used in (b–g). A total of 32 transients were acquired in (a–e), and 128 in (f–g), with the maximum receiver gain in each experiment. The complete experimental parameters are given in the Supporting Information.

fail for molecular identification, very clean spectra are obtained for each species using HD-HAPPY-FESTA (Figure 1c–g). Experimental coupling values were compared with the widely used quantum mechanics density functional theory (DFT) coupling constant calculations.<sup>48–51</sup> The calculated NMR parameters ( $J$  and  $\delta$ ) are routinely applied to support synthetic and natural product structure assignments.<sup>52–55</sup> In our study, DFT was used to support the experimental data by calculating the sign and magnitude of all possible <sup>*n*</sup> $J_{\text{HF}}$ .

## EXPERIMENTAL SECTION

**Sample Preparation.** All reactants and solvents were commercially obtained from Aldrich and were used without

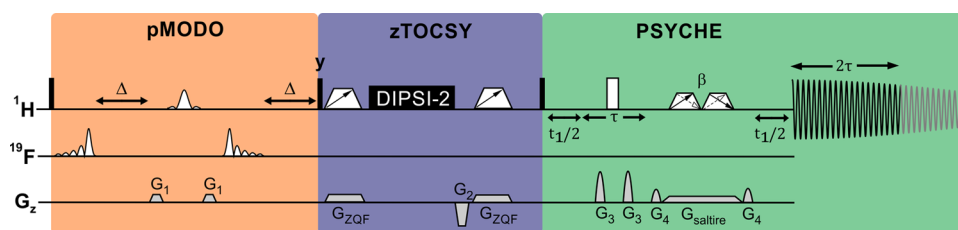


**Figure 2.** Pulse sequence for HD-HAPPY-FESTA. The orange rectangle highlights the selective permuted MODulated echo (pMODO) block, the purple rectangle highlights the zTOCSY block, and the green rectangle the PSYCHE block. Black narrow and white wide rectangles represent hard 90 and 180° pulses, respectively. Trapezoids with cross-diagonal arrows are low-power chirp pulses of small flip angle ( $\beta$ ).<sup>40</sup> Trapezoids on either side of the DIPSI-2 isotropic mixing element<sup>56</sup> are low-power 180° chirp pulses used to suppress zero-quantum coherences.<sup>57</sup> Selective (soft) 180° pulses, represented by shaped pulses, are applied at the resonance frequency of coupled  $^1\text{H}$  and  $^{19}\text{F}$ . Typically, RSNOB or REBURP shapes are used for  $^1\text{H}$  refocus and IBURP2 for  $^{19}\text{F}$  inversion.<sup>58,59</sup>  $\Delta$  is set as  $1/(4 \times n_{\text{F}} \times J_{\text{HF}})$ , where  $J_{\text{HF}}$  is the coupling between  $^1\text{H}$  and  $^{19}\text{F}$  selected by the 180° soft pulses and  $n_{\text{F}}$  is the number of equivalent  $^{19}\text{F}$  selected. A detailed description of the pulse sequence is given in the Supporting Information. Removing the PSYCHE block reduces the dimensionality and increases the sensitivity of the experiment, and the homonuclear couplings are observed (i.e., HAPPY-FESTA).

further purification. Scheme 1 describes the two-step reaction used to prepare all fluorinated molecules, following the synthetic procedure described by Anizelli et al.<sup>46</sup> Commercially available 4-*tert*-butyl-cyclohexanone (**1**) was fluorinated in the  $\alpha$ -ketone position using Selectfluor, which formed the 4-*tert*-butyl-2-fluoro-cyclohexanone isomers (**2a** and **2b**). A total of 92 mg of the crude reaction product of  $\alpha$ -fluorination was dissolved in 600  $\mu\text{L}$  of acetone- $d_6$  and analyzed by NMR without further purification. The remaining crude reaction product was used as a starting material for the second step.  $\text{NaBH}_4$  was used for ketone reduction, generating all four 4-*tert*-butyl-2-fluoro-cyclohexanol isomers (**3a**, **3b**, **3c**, and **3d**) at once. A total of 209 mg of the crude reaction product of ketone reduction was dissolved in 600  $\mu\text{L}$  of  $\text{CDCl}_3$  and analyzed by NMR without further purification.<sup>8</sup> Detailed reaction conditions are fully described in the Supporting Information.

**Data Acquisition and Processing.** All spectra were recorded at 298 K using an 11.4 T Bruker Avance III spectrometer equipped with a 5 mm BBFO smart probe, a QNP switch, and a z-gradient coil with a maximum nominal gradient strength of 53  $\text{G cm}^{-1}$ , operating at 499.87 MHz and 470.35 MHz for  $^1\text{H}$  and  $^{19}\text{F}$ , respectively. All data were processed using the software TopSpin (version 3.5 pl7, Bruker BioSpin). The HAPPY-FESTA experiment duration was approximately 5 min for 2 s of relaxation delay (d1) and 32 transients. The HD-HAPPY-FESTA experiment duration was approximately 2 h 15 min for 2 s of relaxation delay (d1), 32 transients, and 80 chunks. To avoid free induction decay (FID) truncation, the number of pure shift chunks collected was beyond what is needed for a resolution to measure couplings with a precision better than 0.1 Hz. The peak linewidth will ultimately determine the lower limit in  $J$  measurements. The spectra shown here (and in the Supporting Information) were processed with a Lorentz-to-Gauss window function and 128 k points, resulting in a spectral resolution of 0.03 Hz per point after Fourier transform (FT). All raw data, AU macros, and pulse sequence programs used in this paper are available at <https://doi.org/10.25824/redu/LNVQT9> free of charge. Detailed acquisition and processing parameters are described extensively in the Supporting Information (see Figure S1).

**DFT Calculations.** All calculations were performed using the software Gaussian 16<sup>60</sup> by applying the B3LYP hybrid functional.<sup>61–63</sup> The basis set used for geometry optimizations

was the aug-cc-pVTZ,<sup>64</sup> and for the spin–spin coupling constants, the aug-cc-pVTZ-J.<sup>65</sup> Computational details and Cartesian geometries are available in the Supporting Information.

## RESULTS AND DISCUSSION

The NMR pulse sequence for HD-HAPPY-FESTA (Figure 2) is a modification of the conventional MODO-FESTA.<sup>25</sup> Selective pulses on both coupled  $^1\text{H}$  and  $^{19}\text{F}$  are used in a selectively modulated echo, which generates heteronuclear antiphase signals only for the selected spins while refocusing the evolution of all other scalar couplings (see Supporting Information Figure S3b). Following the initial preparation period, a hard 90°  $^1\text{H}$  pulse aided by a zero-quantum filter (ZQF)<sup>57,66</sup> suppression eliminates all signals except for the antiphase component for the selected  $^1\text{H}$ – $^{19}\text{F}$  pair. Using DIPSI-2 as an isotropic mixing element (i.e., TOCSY block),<sup>56</sup> the selected antiphase magnetization is transferred to all other  $^1\text{H}$  spins that are part of the same spin system network (i.e., an unbroken chain of couplings), generating subspectra with heteronuclear antiphase for all  $^1\text{H}$  signals with respect to the selected fluorine (see Supporting Information Figure S3c). As the sense of heteronuclear antiphase is preserved for each signal, the positive/negative signs of each  $J_{\text{HF}}$  are directly observable and are extracted from their relative slope. Lastly, a homonuclear decoupling is achieved using PSYCHE (see Supporting Information Figure S3d).<sup>40</sup> As the resulting spectra are composed of (normally) heteronuclear antiphase doublets, it is less adequate for these spectra to be described as “pure (chemical) shift”, hence these will be referred to as “homonuclear decoupled” spectra. In principle, other pure shift methods could be used for broadband homonuclear decoupling;<sup>67–69</sup> however, PSYCHE generally gives the best sensitivity and spectral purity, and it is the simplest pure shift method for setup and automation.

The modified MODO, described here as “permuted MODO” (pMODO), differs from the conventional MODO in three aspects: (i) the coupling evolution periods ( $\Delta$ , see Figure 2) used here are optimized to maximize antiphase, as opposed to in-phase, contribution; (ii) pMODO uses phase cycling of the hard 90°  $^1\text{H}$  pulse to reinforce the selected coherence transfer pathways (CTP). In conventional MODO, this selection is achieved with differential experiments,<sup>70</sup> which does not apply to antiphase signal selection; and (iii) while in MODO, only a single  $^{19}\text{F}$  pulse is used, in pMODO, two  $^{19}\text{F}$ -

selective inversion pulses are used: a standard pulse and a time-reversed pulse (see Figure 2). Partial  $J_{\text{HF}}$  evolution during the first inversion pulse is refocused during its time-reversed pair,<sup>71</sup> which allows the use of more selective (and longer)  $^{19}\text{F}$  pulses. In conventional MODO, the duration of selective  $^{19}\text{F}$  pulses is restricted to the duration of  $\Delta$ . The narrower a pulse bandwidth, the longer its duration, which causes extra loss of magnetization due to transverse relaxation ( $T_2$ ) and yet it allows the analysis of cognate structures, such as position isomers, where  $^{19}\text{F}$  signals may not be much dispersed.

The products of the  $\alpha$ -fluorination of ketone **1** were analyzed to test the new method. The  $^{19}\text{F}$  spectrum for this mixture (Figure 3a) gives signals that can be used to measure

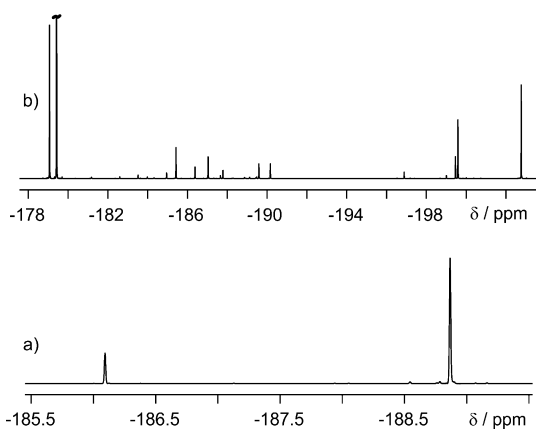
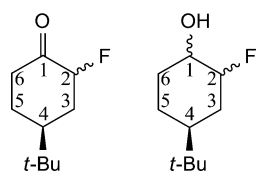


**Figure 3.** 470 MHz  $^{19}\text{F}$  spectra of the crude reaction mixture from: (a)  $\alpha$ -fluorination of ketone **1** in acetone- $d_6$  and (b) reduction of ketones **2a** and **2b** in  $\text{CDCl}_3$ .

the relative quantities of each formed isomer (ketones **2a** or **2b**, the structural motifs are shown in Scheme 2 and 1), but it

#### Scheme 2. Numbered Structural Motifs of (Left) Fluoroketones and (Right) Fluoroalcohols



does not give information about their identity. The many superimposed signals in the conventional and pure shift  $^1\text{H}$  spectra (Figure 4a and b, respectively) prevent characterization, even for this relatively simple mixture, containing mostly product signals. The two deshielded  $^1\text{H}$  signals, at chemical shifts of 5.12 and 4.68 ppm, each with a  $J_{\text{HF}}$  of approximately 50 Hz (as typical for  $^2J_{\text{HF}}$ ), can be attributed as the proton germinal to the fluorine of each ketone, making these signals ideal for HD-HAPPY-FESTA. As for the best setup practice, the less sensitive selective reverse INEPT (SRI)<sup>24,70</sup> can be first used to find exactly the chemical shift of a  $^2J_{\text{HF}}$  proton signal. This was not necessary here. In the first homonuclear-decoupled heteronuclear antiphase  $^1\text{H}$  subspectrum (Figure 4c), three relatively large couplings were measured in the aliphatic  $^1\text{H}$  spectral region: 9.6, 6.7, and 5.4 Hz. Similarly, in the second subspectrum (Figure 4d), the three couplings measured were 41.9, 13.9, and 5.1 Hz. All signals were determined to be positive as all of them had the

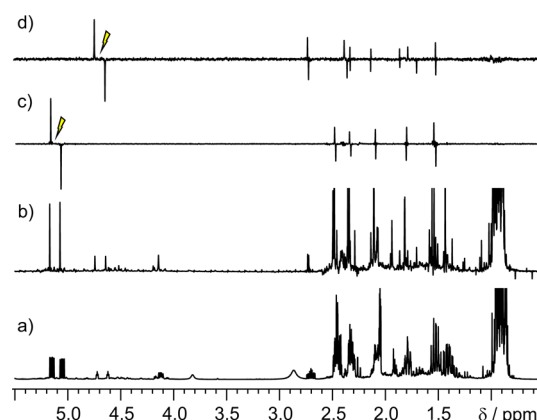


**Figure 4.** 500 MHz (a) conventional, (b) PSYCHE, and (c,d) HD-HAPPY-FESTA (isotropic mixing time of 150 ms)  $^1\text{H}$  spectra of a crude reaction mixture from the  $\alpha$ -fluorination of **1** in acetone- $d_6$ . Ultrahigh-resolution sign-sensitive antiphase heteronuclear total correlation spectra of ketones: (c) **2a** and (d) **2b**, respectively. Molecular structures are shown in Scheme 1. Lightning bolts in (c,d) indicate chemical shifts of band-selective  $^1\text{H}$  pulses, selected using 9.25 ms RSNOB pulses ( $^1\text{H}$  bandwidth of 200 Hz). A flip angle ( $\beta$ ) of  $22^\circ$  and 80 data chunks of 12.5 ms duration were used in (b–d). A total of 32 transients were acquired in (a–d), with the maximum receiver gain in each experiment. The complete experimental parameters are given in the Supporting Information.

same phase as the  $^2J_{\text{HF}}$  proton signal, which is typically largely positive (+ 48.5 and + 50.7 Hz for Figure 4c and d, respectively). The coupling of 41.9 Hz was attributed to the vicinal diaxial  $^3J_{\text{HF}}$  of H3ax in ketone **2b**, identifying ketone **2a** from the subspectrum of Figure 4c, and therefore, ketone **2b** from Figure 4b. Vicinal  $^3J_{\text{HF}}$  values follow similar rules as observed for vicinal  $^3J_{\text{HH}}$  in six-membered ring systems.<sup>72,73</sup> It is not unusual though to observe larger magnitudes for couplings involving fluorine since it is a very electron-rich atom, favoring coupling transmission mechanisms.<sup>47,74,75</sup> Experimental and theoretical coupling constants are in good agreement (see Supporting Information Section C) for both signs and magnitudes. The comparison between the experimental and theoretical data could be used to obtain complementary structural information, easily differentiating between **2a** and **2b**, for example. While in ketone **2a**, the  $^4J_{\text{HF}}$  between axial H4 and equatorial F is approximately  $-1.8$  Hz, and in ketone **2b**, this coupling (with axial F) is  $+1.0$  Hz, agreeing with the DFT-calculated couplings:  $-1.8$  and  $+1.4$  Hz, respectively. This demonstrates how useful for structural characterization the analysis of  $J_{\text{HF}}$  can be, even in positions distant to the probed fluorine, and highlights the importance of determining the sign of coupling constants.

In Figure 5, HAPPY-FESTA and its homonuclear-decoupled version are compared for the spectra of ketone **2b**. One important aspect to be noted is that the homonuclear multiplet structure is the main source of signal overlap in the heteronuclear antiphase subspectrum, as can be seen for the signals between 2.30 and 2.45 ppm shown in Figure 5b and c. It is also obvious that the signal-to-noise ratio (SNR) is severely reduced by the suppression of  $J_{\text{HH}}$  (about 100 times smaller per time unit), as it would for any broadband pure shift NMR method. Despite this, the SNR penalty does not constrict signal identification. The signal amplitude is limited by a short  $T_2$  and a very

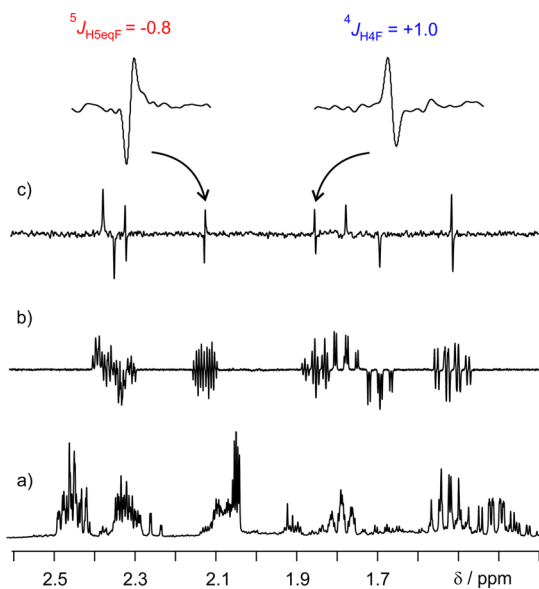


**Figure 5.** Expansion of 500 MHz (a) conventional (expansion of the spectrum shown in Figure 4a), (b) HAPPA-FESTA, and (c) HD-HAPPA-FESTA (expansion of the spectrum shown in Figure 4d)  $^1\text{H}$  spectra of a crude reaction mixture from the  $\alpha$ -fluorination of 4-*tert*-butyl-cyclohexanone in acetone- $d_6$ . Ketone 2b is been observed selectively in (b,c).

small  $J_{\text{HF}}$  (i.e., if signal linewidth is large compared to the magnitude of the coupling, positive and negative edges of the antiphase signal get canceled, reducing the signal intensity), while the furthest heteronuclear coupling measurable is limited by the proton–proton magnetization transfer during the TOCSY block. Heteronuclear couplings as far as  $^5J_{\text{HF}}$  could be measured for the set of molecules studied here. In some cases, where the signal overlap (due to the homonuclear multiplet structure) is not a challenge, HAPPA-FESTA alone should be enough for obtaining sign-sensitive coupling information much quicker than its HD version.

To fully demonstrate the power of HD-HAPPA-FESTA, the crude reaction mixture of the fluorination reaction was used as the starting material for ketone reduction. The  $^{19}\text{F}$  spectrum (Figure 3b) or the  $^1\text{H}$  spectra (conventional spectrum shown in Figure 1a and pure shift spectrum shown in Figure 1b) of such a sample are ineffective for observing the signals belonging to the four alcohol structures. The sundry number of close  $^{19}\text{F}$  signals, with various intensities due to a high-dynamic-range, makes the use of very selective  $^{19}\text{F}$  inversion pulses crucial for the application of FESTA, which are achieved with no difficulty by employing the pMODO block. Here, each alcohol was analyzed first by their  $^3J_{\text{HF}}$  from the carbinolic  $^1\text{H}$  signals, with typical and easy to identify chemical shifts ( $\sim 3.5$  to 4.0 ppm). These measured couplings were 12.1, 7.7, 29.1, and 5.5 Hz for the spectra shown in Figure 1c–f, respectively (the structural motifs are shown in Scheme 1 and 2). This leads to the identification of alcohol 3c for the subspectrum of Figure 1e, as the largest coupling constant (29.1 Hz) is attributed to the diaxial H1–F coupling (26.7 Hz by DFT). Using only this set of couplings for the identification of the remaining molecules is less obvious, as these are all couplings from different axial–equatorial and equatorial–equatorial orientations. The subspectra of Figure 1f also show a very large coupling of 48.0 Hz at 1.49 ppm (i.e., aliphatic region), identifying that as the diaxial  $^3J_{\text{HF}}$  of the axial H3 for the

alcohol 3d, leaving two isomers unidentified. Here is where the DFT results can fully demonstrate support for spectra interpretation. Comparison between the experimental and theoretical results led to the attribution of  $^3J_{\text{HF}}$  of 12.1 and 7.7 Hz to the species 3a and 3b, respectively. The calculated values by DFT were 14.0 and 8.3 Hz. As described for the fluoroketones, the sign of the  $^4J_{\text{HF}}$  of H4 could be used here to differentiate axial (3a–b) from equatorial (3c–d) fluorine cyclohexanols. DFT calculations showed that this coupling is negative when  $^{19}\text{F}$  is at the equatorial position and positive when  $^{19}\text{F}$  is at the axial position, for the compounds studied here. Traditional 2D NMR experiments were not used here as the correlations belonging to minor dilute components are overshadowed by the strong signals of major components, either because of truncation and/or sideband artifacts or due to overlap, and are not adequate for this sort of sample complexity.

Experimental data were further compared with the literature (see Supporting Information Tables S9–S14),<sup>46,76</sup> where purified compounds were studied. Most  $J_{\text{HF}}$  are omitted in these accounts because they are hard to identify even in pure samples, particularly the long-range couplings with a small magnitude. On top of that, most  $^1\text{H}$  chemical shifts are reported as ranges due to signal superposition, which is circumvented here with the use of homonuclear decoupling. As discussed before,  $^1\text{H}$  signals with no (or relatively small)  $J_{\text{HF}}$  that are part of the selected spin system are not observable by HAPPA-FESTA; therefore, their chemical shifts must be extracted from in-phase FESTA experiments. SSE-TOCSY-PSYCHE could also have been used to complement the analysis, but  $^1\text{H}$  signals not coupled to the selected  $^{19}\text{F}$  will potentially cause extra complications if the signals are still superimposed after homonuclear decoupling (see Supporting Information Figure S6).

Other approaches, on the top of the one described here, can be used for recording FESTA. Selective  $^{19}\text{F}$  pulses can be replaced by hard  $180^\circ$   $^{19}\text{F}$  pulses at the cost of spectral purity when selected  $^1\text{H}$  signals are isolated, and a low SNR value is an issue due to transverse relaxation. Another approach for FESTA is replacing MODO by a SRI<sup>24,70</sup> block to provide antiphase coherence selection. SNR is reduced up to twofold in SRI in comparison to MODO (see Supporting Information Figure S4) although spectral purity is often improved. For inspecting very dilute components, the extra sensitivity is welcomed to be sacrificed by the homonuclear decoupling. There are other alternatives described in the literature for the sign-sensitive measurement of heteronuclear couplings. These include the use of 1D-selective HSQC-TOCSY,<sup>77</sup> 2D-selective HSQC-TOCSY,<sup>78</sup> 2D HSQC-TOCSY,<sup>79</sup> and 1D HSQCMBC-CPMG,<sup>69,80</sup> which are normally used in pure compounds and not mixtures. Different nuclei will have different advantages and compromises using either HSQC-based or modulated echo-based experiments. Linear combination of in-phase (IP) and antiphase (AP) signals, with IPAP methods,<sup>81</sup> can also be employed as an alternative to pure shift NMR methods for disentangling heteronuclear from homonuclear coupling contributions; however, differential experiments are prone to subtraction artifacts (i.e., cross-talk signals), relying on very stable magnetic fields. In practice, artifacts are common in both IPAP and pure shift NMR spectra.<sup>82</sup> While the effects of homonuclear couplings, such as  $J$ -modulation to name one, lessen the spectral quality of IPAP, in pure shift NMR, strong

couplings introduce characteristic extra signals in the spectrum, which are shown in the Supporting Information Figure S9.

The long experimental duration for acquiring pure shift experiments ( $\sim 2$  h) can be avoided by combining MODO and HAPPY-FESTA to produce IPAP spectra (under 15 min), but, typically, pure shift spectra will require no further manipulation and are easily interpretable by non-NMR experts.

## CONCLUSIONS

We have demonstrated, for two samples with different complexities, that the novel HD-HAPPY-FESTA method can be used for the direct NMR analysis of fluorinated molecules in crude reaction products. The  $^1\text{H}$  subspectra of spins coupled to a selected  $^{19}\text{F}$  nucleus, extracted with HAPPY-FESTA, unlock the ability to characterize challenging unpurified reaction products, acting as a magnifying glass for dilute fluorine-containing components in a mixture. Heteronuclear couplings ranging from 51.4 to  $-2.3$  Hz could be measured using HD-HAPPY-FESTA, with the smallest measured magnitude of 0.8 Hz. This is the first time (to the best of our knowledge) that selective NMR experiments are used to analyze a completely unfractionated complex reaction mixture, as shown here for the analysis of fluorinated isomers. FESTA is not limited to  $^{19}\text{F}$ , and in principle, it applies to any NMR-active nuclei, such as  $^{31}\text{P}$  or  $^{77}\text{Se}$ . We expect that the new approach finds wide applications not just in synthetic chemistry but also in the fields of medicinal chemistry and biochemistry. In addition, we expect that it may be used by the industry and Academy complementarily to the physical separation methods.

## ASSOCIATED CONTENT

### Supporting Information

The Supporting Information is available free of charge at <https://pubs.acs.org/doi/10.1021/acs.analchem.0c02976>.

Full NMR pulse sequence programs, experimental parameters, synthetic procedures, computational details, additional NMR spectra, and comparison between experimental, theoretical, and literature data (PDF)

## AUTHOR INFORMATION

### Corresponding Author

Guilherme Dal Poggetto – Institute of Chemistry, University of Campinas (UNICAMP), Campinas, São Paulo CEP 13083-970, Brazil; [orcid.org/0000-0003-0591-9166](https://orcid.org/0000-0003-0591-9166); Email: [dalpgt@unicamp.br](mailto:dalpgt@unicamp.br)

### Authors

João Vitor Soares – Institute of Chemistry, University of Campinas (UNICAMP), Campinas, São Paulo CEP 13083-970, Brazil

Cláudio F. Tormena – Institute of Chemistry, University of Campinas (UNICAMP), Campinas, São Paulo CEP 13083-970, Brazil; [orcid.org/0000-0002-1508-0694](https://orcid.org/0000-0002-1508-0694)

Complete contact information is available at:

<https://pubs.acs.org/doi/10.1021/acs.analchem.0c02976>

### Author Contributions

All authors have approved the final version of the manuscript.

### Notes

The authors declare no competing financial interest.

## ACKNOWLEDGMENTS

The authors thank the Fundação de Amparo à Pesquisa do Estado de São Paulo (FAPESP) for providing financial support for this research, through grant No. 2015/08541-6 and a scholarship to G.D.P. (Process No. 2018/19253-0), the Coordenação de Aperfeiçoamento de Pessoal de Nível Superior (CAPES) for a scholarship to J.V.S. (Process No. 88887.339268/2019-00), and the Institute of Chemistry of UNICAMP for the multiuser NMR facility. The authors also gratefully acknowledge Dr. Luis G. T. A. Duarte for providing valuable corrections in this manuscript.

## ADDITIONAL NOTE

<sup>S</sup>The sample was left in the fridge for 6 weeks before analysis as the University was closed due to the COVID-19 crisis.

## REFERENCES

- (1) Shah, P.; Westwell, A. D. *J. Enzyme Inhib. Med. Chem.* **2007**, *22*, 527–540.
- (2) Linclau, B.; Ardá, A.; Reichardt, N. C.; Sollogoub, M.; Unione, L.; Vincent, S. P.; Jiménez-Barbero, J. *Chem. Soc. Rev.* **2020**, 3863.
- (3) Stavber, S.; Zupan, M. *Tetrahedron Lett.* **1996**, *37*, 3591–3594.
- (4) Li, Y.; Xia, G.; Guo, Q.; Wu, L.; Chen, S.; Yang, Z.; Wang, W.; Zhang, Z. Y.; Zhou, X.; Jiang, Z. X. *Med. Chem. Comm.* **2016**, *7*, 1672–1680.
- (5) Aribi, F.; Schmitt, E.; Panossian, A.; Vors, J.-P.; Pazenok, S.; Leroux, F. R. *Org. Chem. Front.* **2016**, *3*, 1392–1415.
- (6) Ichiishi, N.; Caldwell, J. P.; Lin, M.; Zhong, W.; Zhu, X.; Streckfuss, E.; Kim, H. Y.; Parish, C. A.; Krska, S. W. *Chem. Sci.* **2018**, *9*, 4168–4175.
- (7) Wang, J.; Sánchez-Roselló, M.; Aceña, J. L.; del Pozo, C.; Sorochinsky, A. E.; Fustero, S.; Soloshonok, V. A.; Liu, H. *Chem. Rev.* **2013**, *114*, 2432–2506.
- (8) Zhou, Y.; Wang, J.; Gu, Z.; Wang, S.; Zhu, W.; Aceña, J. L.; Soloshonok, V. A.; Izawa, K.; Liu, H. *Chem. Rev.* **2016**, *116*, 422–518.
- (9) Joyce, L. A.; Schultz, D. M.; Sherer, E. C.; Neill, J. L.; Sonstrom, R. E.; Pate, B. H. *Chem. Sci.* **2020**, *11*, 6332.
- (10) Dal Poggetto, G.; Castañar, L.; Morris, G. A.; Nilsson, M. *RSC Adv.* **2016**, *6*, 100063–100066.
- (11) Fräbel, S.; Wagner, B.; Krischke, M.; Schmidts, V.; Thiele, C. M.; Staniek, A.; Warzecha, H. *Metab. Eng.* **2018**, *46*, 20–27.
- (12) Dal Poggetto, G.; Castañar, L.; Adams, R. W.; Morris, G. A.; Nilsson, M. *Chem. Commun.* **2017**, *53*, 7461–7464.
- (13) Dal Poggetto, G.; Castañar, L.; Adams, R. W.; Morris, G. A.; Nilsson, M. *J. Am. Chem. Soc.* **2019**, *141*, 5766–5771.
- (14) Moutzouri, P.; Kiraly, P.; Phillips, A. R.; Coombes, S. R.; Nilsson, M.; Morris, G. A. *Chem. Commun.* **2017**, *53*, 123–125.
- (15) Gilard, V.; Balayssac, S.; Tinaugus, A.; Martins, N.; Martino, R.; Malet-Martino, M. *J. Pharm. Biomed. Anal.* **2015**, *102*, 476–493.
- (16) Power, J. E.; Foroozandeh, M.; Adams, R. W.; Nilsson, M.; Coombes, S. R.; Phillips, A. R.; Morris, G. A. *Chem. Commun.* **2016**, *52*, 2916–2919.
- (17) Mistry, N.; Ismail, I. M.; Farrant, R. D.; Liu, M.; Nicholson, J. K.; Lindon, J. C. *J. Pharm. Biomed. Anal.* **1999**, *19*, 511–517.
- (18) Dal Poggetto, G.; Favaro, D. C.; Nilsson, M.; Morris, G. A.; Tormena, C. F. *Magn. Reson. Chem.* **2014**, *52*, 172–177.
- (19) Power, J. E.; Foroozandeh, M.; Moutzouri, P.; Adams, R. W.; Nilsson, M.; Coombes, S. R.; Phillips, A. R.; Morris, G. A. *Chem. Commun.* **2016**, *52*, 6892–6894.
- (20) Dalvit, C.; Vulpetti, A. *J. Med. Chem.* **2018**, *62*, 2218–2244.
- (21) Foli, G.; Degli Esposti, M.; Toselli, M.; Morselli, D.; Fabbri, P. *Analyst* **2019**, *144*, 2087–2096.
- (22) Chen, H.; Viel, S.; Ziarelli, F.; Peng, L. *Chem. Soc. Rev.* **2013**, *42*, 7971–7982.
- (23) Yu, M.; Xie, D.; Kadakia, R. T.; Wang, W.; Que, E. L. *Chem. Commun.* **2020**, *56*, 6257–6260.

- (24) Castañar, L.; Moutzouri, P.; Barbosa, T. M.; Tormena, C. F.; Rittner, R.; Phillips, A. R.; Coombes, S. R.; Nilsson, M.; Morris, G. A. *Anal. Chem.* **2018**, *90*, 5445–5450.
- (25) Barbosa, T. M.; Castañar, L.; Moutzouri, P.; Nilsson, M.; Morris, G. A.; Rittner, R.; Tormena, C. F. *Anal. Chem.* **2020**, *92*, 2224–2228.
- (26) Braunschweiler, L.; Ernst, R. R. *J. Magn. Reson.* **1983**, *53*, 521–528.
- (27) Macheteau, J.-P.; Oulyadi, H.; Van Hemelryck, B.; Bourdonneau, M.; Davoust, D. *J. Fluorine Chem.* **2000**, *104*, 149–154.
- (28) Luy, B.; Barchi, J. J., Jr.; Marino, J. P. *J. Magn. Reson.* **2001**, *152*, 179–184.
- (29) Stockwell, J.; Daniels, A. D.; Windle, C. L.; Harman, T. A.; Woodhall, T.; Lebl, T.; Trinh, C. H.; Mulholland, K.; Pearson, A. R.; Berry, A.; Nelson, A. *Org. Biomol. Chem.* **2016**, *14*, 105–112.
- (30) Battiste, J.; Newmark, R. *Prog. Nucl. Magn. Reson. Spectrosc.* **2006**, *48*, 1–23.
- (31) Hennig, M.; Munzarová, M. L.; Bermel, W.; Scott, L. G.; Sklenář, V.; Williamson, J. R. *J. Am. Chem. Soc.* **2006**, *128*, 5851–5858.
- (32) Davis, D. G.; Bax, A. *J. Am. Chem. Soc.* **1985**, *107*, 7197–7198.
- (33) Kessler, H.; Oschkinat, H.; Griesinger, C.; Bermel, W. *J. Magn. Reson.* **1986**, *70*, 106–133.
- (34) Dalvit, C.; Bovermann, G. *Magn. Reson. Chem.* **1995**, *33*, 156–159.
- (35) Espinosa, J. F. *J. Org. Chem.* **2013**, *78*, 12844–12847.
- (36) Espinosa, J. F.; Broughton, H. *Eur. J. Org. Chem.* **2013**, *2013*, 6972–6978.
- (37) Aguilar, J. A.; Morris, G. A.; Kenwright, A. M. *RSC Adv.* **2014**, *4*, 8278–8282.
- (38) Chaudhari, S. R.; Suryaprakash, N. *RSC Adv.* **2014**, *4*, 15018–15021.
- (39) Lokesh, N.; Sachin, S. L.; Mishra, S. K.; Suryaprakash, N. *Chem. Phys. Lett.* **2015**, *640*, 157–160.
- (40) Foroozandeh, M.; Adams, R. W.; Meharry, N. J.; Jeannerat, D.; Nilsson, M.; Morris, G. A. *Angew. Chem., Int. Ed.* **2014**, *53*, 6990–6992.
- (41) Foroozandeh, M.; Adams, R. W.; Nilsson, M.; Morris, G. A. *J. Am. Chem. Soc.* **2014**, *136*, 11867–11869.
- (42) Foroozandeh, M.; Castañar, L.; Martins, L. G.; Sinnaeve, D.; Dal Poggetto, G.; Tormena, C. F.; Adams, R. W.; Morris, G. A.; Nilsson, M. *Angew. Chem., Int. Ed.* **2016**, *55*, 15579–15582.
- (43) Adams, R. W. *eMagRes* **2014**, *86-87*, 295–220.
- (44) Castañar, L.; Parella, T. *Magn. Reson. Chem.* **2015**, *53*, 399–426.
- (45) Zangger, K. *Prog. Nucl. Magn. Reson. Spectrosc.* **2015**, *86-87*, 1–20.
- (46) Anizelli, P. R.; Favaro, D. C.; Contreras, R. H.; Tormena, C. F. *J. Phys. Chem. A* **2011**, *115*, 5684–5692.
- (47) Viesser, R. V.; Ducati, L. C.; Autschbach, J.; Tormena, C. F. *Phys. Chem. Chem. Phys.* **2016**, *18*, 24119–24128.
- (48) Bifulco, G.; Dambruoso, P.; Gomez-Paloma, L.; Riccio, R. *Chem. Rev.* **2007**, *107*, 3744–3779.
- (49) Lodewyk, M. W.; Siebert, M. R.; Tantillo, D. J. *Chem. Rev.* **2012**, *112*, 1839–1862.
- (50) Grimme, S.; Bannwarth, C.; Dohm, S.; Hansen, A.; Pisarek, J.; Pracht, P.; Seibert, J.; Neese, F. *Angew. Chem., Int. Ed.* **2017**, *56*, 14763–14769.
- (51) Krivdin, L. B. *Prog. Nucl. Magn. Reson. Spectrosc.* **2018**, *108*, 17–73.
- (52) Navarro-Vázquez, A.; Gil, R. R.; Blinov, K. *J. Nat. Prod.* **2018**, *81*, 203–210.
- (53) Castro, S. J.; García, M. E.; Padrón, J. M.; Navarro-Vázquez, A.; Gil, R. R.; Nicotra, V. E. *J. Nat. Prod.* **2018**, *81*, 2329–2337.
- (54) Farley, K. A.; Che, Y.; Navarro-Vázquez, A.; Limberakis, C.; Anderson, D.; Yan, J.; Shapiro, M.; Shanmugasundaram, V.; Gil, R. R. *J. Org. Chem.* **2019**, *84*, 4803–4813.
- (55) Koos, M. R. M.; Navarro-Vázquez, A.; Anklin, C.; Gil, R. R. *Angew. Chem., Int. Ed.* **2020**, *59*, 3938–3941.
- (56) Rucker, S. P.; Shaka, A. J. *Mol. Phys.* **2006**, *68*, 509–517.
- (57) Thrippleton, M. J.; Keeler, J. *Angew. Chem., Int. Ed.* **2003**, *42*, 3938–3941.
- (58) Geen, H.; Freeman, R. *J. Magn. Reson.* **1991**, *93*, 93–141.
- (59) Kupče, Ě.; Boyd, J.; Campbell, I. D. *J. Magn. Res. Ser. B* **1995**, *106*, 300–303.
- (60) Frisch, M. J.; Trucks, G. W.; Schlegel, H. B.; Scuseria, G. E.; Robb, M. A.; Cheeseman, J. R.; Scalmani, G.; Barone, V.; Petersson, G. A.; Nakatsuji, H.; Li, X.; Caricato, M.; Marenich, A. V.; Bloino, J.; Janesko, B. G.; Gomperts, R.; Mennucci, B.; Hratchian, H. P.; Ortiz, J. V.; Izmaylov, A. F., et al. *Gaussian 16*, revision B.01; 2017.
- (61) Becke, A. D. *Phys. Rev. A* **1988**, *38*, 3098–3100.
- (62) Becke, A. D. *J. Chem. Phys.* **1993**, *98*, 5648–5652.
- (63) Krivdin, L. B. *Magn. Reson. Chem.* **2019**, *57*, 897–914.
- (64) Woon, D. E.; Dunning, T. H., Jr. *J. Chem. Phys.* **1993**, *98*, 1358–1371.
- (65) Provasi, P. F.; Aucar, G. A.; Sauer, S. P. A. *J. Chem. Phys.* **2001**, *115*, 1324–1334.
- (66) Koivisto, J. J. *Chem. Commun.* **2013**, *49*, 96–98.
- (67) Zangger, K.; Sterk, H. *J. Magn. Reson.* **1997**, *124*, 486–489.
- (68) Mauhart, J.; Glanzer, S.; Sakhaei, P.; Bermel, W.; Zangger, K. *J. Magn. Reson.* **2015**, *259*, 207–215.
- (69) Timári, I.; Kövér, K. E. *Magn. Reson. Chem.* **2018**, *56*, 910–917.
- (70) Freeman, R.; Mareci, T. H.; Morris, G. A. *J. Magn. Reson.* **1981**, *42*, 341–345.
- (71) Kupče, Ě.; Freeman, R. *J. Magn. Reson.* **1997**, *127*, 36–48.
- (72) Contreras, R. n. H.; Peralta, J. E. *Prog. Nucl. Magn. Reson. Spectrosc.* **2000**, *37*, 321–425.
- (73) Williamson, K. L.; Hsu, Y.-F. L.; Swager, S.; Hall, F. H.; Coulter, M. S. *J. Am. Chem. Soc.* **1968**, *90*, 6717–6722.
- (74) Krivdin, L. B.; Contreras, R. H. *In Ann. Reports on NMR spec.* **2007**, *133–245*.
- (75) Hierso, J. C. *Chem. Rev.* **2014**, *114*, 4838–4867.
- (76) Graton, J.; Wang, Z.; Brossard, A. M.; Goncalves Monteiro, D.; Le Questel, J. Y.; Linclau, B. *Angew. Chem., Int. Ed.* **2012**, *51*, 6176–6180.
- (77) Sauri, J.; Nolis, P.; Parella, T. *J. Magn. Reson.* **2013**, *236*, 66–69.
- (78) Sauri, J.; Espinosa, J. F.; Parella, T. *Angew. Chem., Int. Ed.* **2012**, *51*, 3919–3922.
- (79) Sauri, J.; Nolis, P.; Parella, T. *Magn. Reson. Chem.* **2015**, *53*, 427–432.
- (80) Timári, I.; Illyés, T. Z.; Adams, R. W.; Nilsson, M.; Szilágyi, L.; Morris, G. A.; Kövér, K. E. *Chem. – Eur. J.* **2015**, *21*, 3472–3479.
- (81) Castañar, L.; Sauri, J.; Williamson, R. T.; Virgili, A.; Parella, T. *Angew. Chem., Int. Ed.* **2014**, *53*, 8379–8382.
- (82) Sauri, J.; Parella, T. *Magn. Reson. Chem.* **2013**, *51*, 509–516.